Published in final edited form as:
Macromolecules. 2007 ; 40(25): 8833–8841. doi:10.1021/ma071659t.

Enhanced Luminescence from Emissive Defects in Aggregated Conjugated Polymers

Andrew Satrijo, **Steven E. Kooi**, and **Timothy M. Swager***
Department of Chemistry and The Institute for Soldier Nanotechnologies, Massachusetts Institute of Technology, Cambridge, Massachusetts 02139

Abstract

Degradation experiments and model studies suggested that the longer lived green fluorescence from an aggregated poly(*p*-phenylene ethynylene) (PPE) was due to the presence of highly emissive, low-energy, anthryl defect sites rather than the emissive conjugated polymer excimers proposed in a previous report. After elucidating the origin of the green fluorescence, additional anthryl units were purposely incorporated into the polymer to enhance the blue-to-green fluorescence color change that accompanied polymer aggregation. The improved color contrast from this anthryl-doped conjugated polymer led to the development of crude solution-state and solid-state sensors, which, upon exposure to water, exhibited a visually noticeable blue-to-green fluorescence color change.

Introduction

One of the most widely studied applications for conjugated polymers is in light-emitting diodes.[1] Robust polymer light emitting diodes (PLEDs) with sufficiently long working lifetimes have been assembled using π–conjugated polymers that emit green, red, and yellow light; however, constructing a PLED with a stable, blue-emitting polymer film still remains a formidable challenge.[2] One of the most popular classes of conjugated polymers for blue PLEDs is polyfluorene and its derivatives.[3,4] However, the stability and working lifetime of these conjugated polymers are still limited. Under normal operating conditions, the light emission from poly(9,9-dialkylfluorene) PLEDs can change in color from the desired blue to an unwanted green. The new, low-energy, green band in the polyfluorene emission spectrum was initially attributed to the formation of emissive aggregates and/or excimers.[5,6] Typically, excimers are spectroscopically characterized by broad, vibrationally unstructured, low-energy emission bands with long excited-state lifetimes.[7,8]

In addition to polyfluorene, conjugated polymer excimers have also been previously reported[9] in heterocyclic, rigid-rod conjugated polymers,[10-12] ladder-type poly(*p*-phenylene)s,[13] and cyano-substituted poly(*p*-phenylene vinylene)s.[14] Recently, our group reported the synthesis of highly emissive conjugated polymer excimers based on poly(*p*-phenylene ethynylene) (PPE) containing [2.2.2] bicyclic ring systems having an alkene bridge substituted with ester groups, labeled in Figure 1 as *anti*-PPE and *syn*-PPE.[15] When *anti*-PPE was dissolved in dilute chloroform solution, the polymer chains were isolated from each other, so the emission spectrum was dominated by the inherent short-wavelength (0,0) emission of the polymer around 432 nm and the accompanying (0,1) emission at 459 nm. Emission at these wavelengths made the solution appear fluorescent blue when irradiated with ultraviolet light. However, when *anti*-PPE was aggregated in a concentrated solution, a multilayer thin film, or a spin-cast film, it exhibited a new, broad, longer lived, low-energy (~496 nm), green emission

* Corresponding author. E-mail: E-mail: tswager@mit.edu.

band. As the thickness of the spin-cast film increased, the emission intensity of the green band increased relative to the inherent blue emission of the polymer. This effect was attributed to two factors. First, thicker films would have a greater probability of excimer formation since there would be a higher ratio of polymer–polymer interfaces relative to polymer–air and polymer–substrate interfaces. Second, thicker films would have enhanced exciton migration from high-energy sites (e.g., polymer chain segments) to low-energy sites (e.g., excimers). This phenomenon arises from migrating excitons being more efficient, according to random-walk statistics, at sampling a larger number of different sites in thick three-dimensional films than in thin two-dimensional films.[16] In the present study, we investigated this phenomenon of aggregation-enhanced exciton migration in conjugated polymers, and we studied how it led to amplified green emissions from these PPE films.

The origin of the low-energy, green emission bands in various conjugated polymer films have been under much debate over the past few years. Several groups have recently argued that the green bands in the polyfluorene emission spectrum were actually not due to the presence of emissive conjugated polymer aggregates or excimers, but due to the formation of emissive on-chain defects.[17-29] It has been proposed that polyfluorenes can easily undergo oxidative degradation, resulting in the formation of fluorenone defects sites on the polymer chain.

Since conjugated polymer films are very efficient at funneling excitons from high-energy sites (e.g., the blue-emitting fluorene segments) to low-energy sites (e.g., the green-emitting fluorenone defects), only a small concentration of low-energy defect sites is necessary to effectively alter the polymer film emission from blue to green. This efficient exciton transport[16,30,31] in conjugated polymer films makes them very sensitive to the presence of emissive defects, emission-quenching defects, and emission-quenching analytes targeted for sensor applications.[32-34] Therefore, we decided to further investigate the origin of the green emission bands from films of PPEs containing [2.2.2] bicyclic ring systems having an alkene bridge substituted with ester groups. We examined whether the green emission actually originated from excimers, as originally proposed,[15] or from emissive defects similar to those in polyfluorene systems.

Results and Discussion

Preliminary Degradation Studies

One of the biggest limitations of implementing organic materials in semiconductor devices is the limited stability of many organic structures, leading to short working lifetimes relative to inorganic materials, such as silicon, which forms a protective oxide coating upon oxidation.[2,35] Although this stability problem is well known in the field of conjugated polymers, it is still commonly overlooked. To investigate whether the green emission from films of *anti*-PPE originated from excimers or emissive defects formed by degradation, we characterized the polymer before and after purposely degrading it (Figure 2). First, *anti*-PPE (M_n = 39 kDa) was resynthesized according to a previously reported procedure.[36] Then spin-cast films of the polymer were subjected to photodegradation in an ambient air atmosphere or in an inert nitrogen atmosphere. Both types of light exposure resulted in enhancements of the green band fluorescence intensity relative to the inherent blue (0,0) emission of the polymer (around 439 nm). For thermal degradation studies, a bulk sample of *anti*-PPE was heated to 300 °C in an inert helium atmosphere using a thermogravimetric–mass spectrometer (*vide infra*). The degraded polymer was then dissolved in chloroform, filtered, and then spin-cast into a film. Similar to those of the photodegraded polymer films, the fluorescence spectrum of the thermally degraded polymer also showed an enhanced emission intensity of the green band relative to the inherent blue (0,0) emission of the polymer (around 440 nm).

The degradation experiments demonstrated that the green emission from the polymer film can be enhanced by simply decomposing the polymer by photoirradiation or by thermal degradation. This demonstration suggested that the green bands may actually originate from emissive defect sites rather than emissive aggregates or excimers.

Simulating a Degraded Polymer

To elucidate the identity of the green-emitting defect species, we synthesized several other PPEs. A spin-cast film of *syn*-PPE (28 kDa) had an emission spectrum (Figure 3) exhibiting a green band that was red-shifted by about 52 nm from the inherent short-wavelength (0,0) emission band of the polymer, similar to the emission spectrum of the *anti*-PPE film. Therefore, the green-emitting defect species existed in both *anti*-PPE and *syn*-PPE, and the green band emission was not unique to a specific molecular geometry. Analogous to *anti*-PPE, when we thermally degraded *syn*-PPE, filtered it, and then spin-cast the polymer into a film, its emission spectrum exhibited a green band with enhanced relative intensity (*vide infra*).

Both *anti*-PPE and *syn*-PPE contain [2.2.2] bicyclic ring systems having alkene bridges substituted with ester groups, formed by two Diels–Alder reactions between **1** and dimethyl acetylenedicarboxylate (DMAD). Our group previously proposed that the [2.2.2] ring system containing an alkene bridge substituted with ester groups was pivotal to excimer formation.[15] Our group has also synthesized PPEs that contain [2.2.2] bicyclic ring systems formed by Diels–Alder reactions between an anthracene moiety and either *N*-methylmaleimide or *N*-phenylmaleimide.[37] Notably, these polymers were proposed to undergo retro-Diels–Alder reactions upon heating above 210 °C in an inert nitrogen atmosphere (Figure 4). The product of the retro-Diels–Alder reaction contained anthracene moieties conjugated to the PPE main chain. The new anthryl units provided additional electronic delocalization that would lead to lower-energy electronic transitions in the polymer. As a result, solutions of the thermally reacted conjugated polymer fluoresced at longer wavelengths than solutions of the unheated PPE.

The thermal reactivity of these [2.2.2] bicyclic ring systems suggested that the *anti*-PPE and *syn*-PPE polymers may also undergo C–C bond cleavage at the 9,10-positions to produce similar anthracene-containing defect sites (Figure 5).

To elucidate the degradation mechanism of these polymers, thermogravimetric–mass spectrometry (TG–MS) studies were performed (see Supporting Information). These experiments suggested that the thermal degradation might not involve a simple retro-Diels–Alder mechanism, but instead, may involve a more complicated decomposition pathway.

To construct a model of the proposed, anthacene-containing, degraded polymer, we first synthesized an anthryl comonomer **3**, which we then added into the Sonogashira–Hagihara cross-coupling polymerization in various comonomer ratios (Scheme 1).

The resulting statistical copolymer, doped with various amounts of anthryl comonomer, was named *syn*-PPE$_y$, where the subscript *y* denotes the molar percentage of anthryl dopants **3** of the total diacetylene comonomers (***syn*-4 + 3**) added into the polymerization reaction. The ^{1}H NMR spectra of the doped polymers, *syn*-PPE$_y$, as well as the undoped *syn*-PPE, all showed low-intensity signals in the δ 8.12−7.55 ppm aromatic region (Figures S.1–6 in the Supporting Information) that generally increased in relative abundance as the percentage of anthryl comonomer increased. These low-intensity, aromatic, impurity signals were also observed in the ^{1}H NMR spectra of *anti*-PPE (Figures S.7–8), which was consistent with the NMR spectrum previously obtained for the same polymer.[38] Table 1 shows that the integration ratio, *R* (8.1/6.0), of the low-intensity aromatic proton signal around 8.1 ppm to the bridgehead proton signal (around 6.0 ppm), increased as the amount of anthryl dopant increased.

The NMR spectra of the thermally degraded (300 °C) *anti*-PPE (Figures S.9–10) had an *R* (8.1/6.0) value of 0.029, which is characteristic of the anthryl-doped PPEs. Degradation at such a high temperature also resulted in additional impurity signals around δ 1.7−0.8 ppm due to the generation of other decomposition products from side reactions (e.g., chain cleavage). Thus, a 10% decrease in the number-average molecular weight, M_n, of the polymer also accompanied the degradation (Table 1). When *syn*-PPE was similarly degraded under an inert helium atmosphere, but at a slightly lower temperature (250 °C), the NMR spectra (Figures S.11–12) of the degraded polymer appeared similar, with an *R*(8.1/6.0) value of 0.039. However, since the aromatic impurities in the polymers were present in relatively small amounts, it was difficult to quantify them accurately. To help identify the aromatic impurity, the optical properties of the polymers were compared. The absorption and emission spectra of the *syn*-PPE_y copolymers and the thermally degraded *syn*-PPE are shown in Figure 6 and summarized in Table 2.

The optical effects of incorporating anthracene groups into the polymer backbone of a PPE had been previously studied.[39] These studies showed that the addition of small comonomer concentrations (7%) of anthracene groups resulted in emission spectra with new, intense, long-wavelength emission bands. The results of this previously reported study were consistent with the emission spectra of the synthesized *syn*-PPE_y, which also contained small concentrations of anthryl dopants.

Compared to that of the undoped *syn*-PPE, the film of *syn*-PPE_1 exhibited a green emission band with significantly greater relative intensity (I_{green}/I_{blue} = 1.6 and 3.2, respectively) due to the presence of the additional anthryl units. Furthermore, *syn*-PPE and *syn*-PPE_1 appeared to have comparable excited state lifetimes in both solutions and films. This suggested that the low-energy anthryl sites in *syn*-PPE_1 were responsible for the long (1.5–1.9 ns) excited state lifetimes observed in the films' green emission region. Therefore, the long excited state lifetime (1.5 ns) observed in the undoped *syn*-PPE film was unlikely due to the presence of excimers.

As expected, the film of *syn*-PPE_9 had an emission spectrum that was dominated by the green emission band (I_{green}/I_{blue} = 46). At such a high anthryl comonomer dopant level of 9%, even dilute chloroform solutions of *syn*-PPE_9 exhibited a noticeable green band emission (at 507 nm). The green band emission of the solution also had a long excited state lifetime component (1.8 ns), supporting that anthryl units were responsible for the long-lived, low-energy excited states. The long excited state lifetime of the low-energy species relative to that of the high-energy species (e.g., the blue-emitting PPE segments) is characteristic of energy-funneling in conjugated polymers.[16, 30]

When *syn*-PPE was thermally degraded at 250 °C in an inert helium atmosphere, it exhibited similar spectral characteristics (Figure 6c) as those of *syn*-PPE_9 (Figure 6b). Solutions of both the thermally degraded *syn*-PPE and *syn*-PPE_9 emitted a distinct, long-lived, green band around 507–511 nm. Both solutions also showed a noticeable shoulder above 450 nm in the absorption spectra, which can be attributed to the absorption of the anthryl unit conjugated to the PPE backbone. In agreement, the (unconjugated) anthryl monomer, **3**, also exhibited a red-shifted absorption spectrum relative to those of the ***anti*-4** and ***syn*-4** monomers, due to the additional electronic delocalization provided by the aromatic anthracene moiety (Figure 7).

Excitation of both solutions of the thermally degraded *syn*-PPE and *syn*-PPE_9 with low-energy (459 nm) photons resulted in emission spectra exhibiting only one distinct band around 507–511 nm (Figure 8). The lack of a (0,1) fluorescence band or shoulder (at wavelengths below 480 nm) showed that the low-energy, 459 nm photons could not photoexcite the PPE chains to any considerable extent. These spectral features suggested that the luminophores responsible for the green emission bands can be directly excited from an electronic ground state, which does not exist in an excimer.[7]

The thermally degraded *anti*-PPE also exhibited similar spectral properties in the film state (Figure 2b) and in the solution state (Figure 9). As expected, the emission spectra of the solution also revealed a low-energy green band at 512 nm, which could be directly excited by photoirradiation at 459 nm. Therefore, the green-emitting species in these polymers can be excited either indirectly by energy transfer from a higher-energy species (e.g., photoexcited PPE chain segments) or directly by low-energy (459 nm) photoirradiation. The spectral similarities between the thermally degraded undoped PPEs and the anthryl-doped *syn*-PPE_9 supported that the unknown, long-lived, green-emitting species are, in fact, anthryl defect sites.

The formation of small quantities of anthryl defect sites in the PPE chain may have occurred during the polymerization reaction, which required heating at elevated temperatures (70 °C) for 3 days. Unfortunately, conjugated polymers that are susceptible to such degradation will inevitably vary in purity between different samples, making accurate quantitative comparisons difficult.

Aggregation Studies

The green band emission from the PPEs are much more pronounced when the polymers were in their film state than when they were dissolved in dilute solutions. This observation was due to the enhanced exciton migration present in conjugated polymer films relative to that in dilute, well-dissolved polymer solutions. In a dilute chloroform solution, only *intra*chain exciton migration was possible because the polymer chains were isolated from each other. However, in the film state, the conjugated polymer chains were aggregated within close proximity to each other so *inter*chain exciton migration also became possible. The three-dimensional random walk available to an exciton in a polymer film enabled the exciton to sample a much greater number of different sites than by the one-dimensional random walk available to an exciton in dilute, well-dissolved, polymer solutions.[16,40] Therefore, an exciton in a conjugated polymer is much more likely to find a low-energy exciton trap site if the polymer is in its solid film state than in a dilute solution state. If the low-energy exciton trap sites are emissive, such as the anthryl defect sites investigated in this study, then they can dramatically alter the emission spectra of polymers in their film state; however, they may go unnoticed in the emission spectra of dilute, well-dissolved, polymer solutions.

To further investigate the effects of exciton migration on luminescence properties, we conducted absorption and fluorescence spectroscopy on PPE solutions in various degrees of aggregation. By adding a poor solvent (i.e., a solvent in which the polymer is in a collapsed or aggregated state) to a PPE solution dissolved in a good solvent (i.e., a solvent in which the polymer is in an expanded and well-dissolved state),[41] it was possible to study the polymers in various degrees of aggregation (Figure 10). In dilute THF solutions, the polymers were well dissolved and isolated. Since only *intra*chain exciton migration was possible, and the small concentration of emissive exciton traps are not noticeable in the fluorescence spectra. Thus, both THF solutions of *syn*-PPE and *syn*-PPE_1 appeared fluorescent blue, as characterized by the sharp emission band around 432–434 nm and the green emission bands are absent. However, in the 50:50 THF:H_2O cosolvent mixtures, the polymers were present in aggregated states, held together by hydrophobic and π–π interactions. Upon aggregation, *inter*chain exciton migration became significant, so the emissive exciton traps noticeably altered the fluorescence spectra, exhibiting a dominant green emission band around 513 nm. As expected, the fluorescence spectra of the *syn*-PPE_1 aggregate solution had a greater I_{green}/I_{blue} ratio than that of *syn*-PPE (1.50 and 1.15, respectively) because of the additional anthryl sites present in *syn*-PPE_1. As shown by the fluorescence photographs in Figure 10, the additional anthryl units led to a more noticeable blue-to-green fluorescence color change in solutions of *syn*-PPE_1 than in solutions of *syn*-PPE.

Since *syn*-PPE_1 demonstrated a noticeable blue-to-green fluorescence color change in the solution state, we then investigated the fluorescence color change of this polymer when it was dispersed in a solid poly(vinyl alcohol) (PVA) matrix. PVA is a water-soluble polymer that has been widely used to make water-permeable hydrogels.[42,43] To disperse the PPE into a matrix of PVA, we quickly added a (fluorescent blue) PPE/THF solution into an aqueous solution of PVA. The resulting polymer blend immediately began to precipitate out of the 70:30 THF:H_2O cosolvent mixture. While rapidly stirring the mixture, a drop of 50 wt% glutaric dialdehyde was quickly added to help crosslink the PVA chains. A fluorescent greenish blue polymer solid was removed from the mixture, and then characterized by fluorescence spectroscopy (Figure 11, red line). The polymer blend was then washed in 100% THF to remove the small amount of water from the polymer and disperse the PPE chains within the PVA matrix. After the THF wash, the polymer blend became fluorescent blue, and remained so even after drying *in vacuo* (Figure 11, blue line).

To induce a fluorescence color change, the polymer blend was submerged into pure water for two minutes. The observed blue-to-green fluorescence color change (Figure 11, green line) was attributed to the water-induced aggregation of the PPE chains within the PVA matrix. When the polymer blend was dried *in vacuo*, it remained fluorescent green. Unfortunately, the fluorescence color change was not reversible when the polymer blend was put into THF because of the difficulty of separating the polymer chains once they became strongly aggregated in 100% water.

The addition of emissive, low-energy, exciton trap sites into *syn*-PPE improved the contrast of the fluorescence color change of the polymer undergoing aggregation. This improvement led to the development of crude solution-state and solid-state sensors displaying a visually noticeable fluorescent color change upon exposure to water. These responsive materials demonstrated how aggregation (and, thus, improved exciton migration) in conjugated polymers can lead to enhanced luminescence from emissive exciton trap sites.

Conclusions

In summary, degradation experiments and model studies were performed to investigate the origin of the green bands in the solid-state fluorescence spectra of poly(*p*-phenylene ethynylene)s containing [2.2.2] bicyclic ring systems having an alkene bridge substituted with ester groups. These experiments suggested the green fluorescence band may be due to the presence of highly emissive, low-energy, anthryl defect sites rather than the emissive excimers that were previously proposed.[15] After elucidating the origin of the green fluorescence, we then improved the blue-to-green fluorescence color contrast of the polymer undergoing aggregation by purposely adding more of the anthryl exciton trap sites into the conjugated polymer. This improvement led to the development of crude solution-state and solid-state sensors, which, upon exposure to water, underwent a visually noticeable fluorescence color change.

Experimental Section

General Methods and Instrumentation

All air- or moisture-sensitive synthetic manipulations were carried out under an inert nitrogen or argon atmosphere using standard Schlenk techniques or in an inert-atmosphere glovebox (Innovative Technology, Inc.). ^{1}H NMR spectra were recorded on either a Varian 300 MHz or a Varian 500 MHz NMR spectrometer. Chemical shifts of each signal are reported in units of δ (ppm) and referenced to the residual signal of the solvent (chloroform-d: 7.27 for ^{1}H, 77.23 for ^{13}C). Splitting patterns are designated as s (singlet), d (doublet), t (triplet), q (quartet), m (multiplet), and br (broad). High-resolution mass spectra (HRMS) were obtained at the MIT

Department of Chemistry Instrumentation Facility on a Bruker Daltonics APEX II 3 Tesla FT–ICR–MS using electrospray ionization (ESI). Gas chromatography–mass spectrometry (GC–MS) was performed on an Agilent 5973N Gas Chromatograph/Mass Spectrometer (Agilent Technologies, Inc.) with a Restek Rtx-1 column (30.0 m × 250 μm × 1.00 μm), an inlet temperature of 250 °C, and a helium flow rate of 1.0 mL/min. The oven temperature was set at 100 °C for 5 min, then ramped at 20 °C/min to 250 °C, held for 5 min, ramped at 30 °C/min to 320 °C, then held for 8 min. Melting points (mp) were measured with a Mel-Temp II (Laboratory Devices). Thermogravimetric–mass spectrometry (TG–MS) was performed on a TGA Q50 (TA Instruments) coupled to a ThermoStar Gas Analysis System GSD 301 T3 (Pfeiffer Vacuum) with a helium flow rate of 90 mL/min and a furnace temperature ramp of 5 °C/min. Gases were analyzed with a 1–300 amu quadrupole mass analyzer (QMA) with an electron impact ionization source. Attenuated total reflection infrared (ATR–IR) spectra were obtained on a NEXUS 870 spectrometer.

Polymer molecular weights were determined by gel permeation chromatography (GPC) versus polystyrene standards (Agilent Technologies, Inc.) using THF as the eluent at a flow rate of 1.0 mL/min in a Hewlett Packard series 1100 GPC system equipped with three PLgel 5 μm 10^5, 10^4, 10^3 (300 × 7.5 mm) columns in series and a diode array detector at 254 nm.

The UV–vis absorption and fluorescence spectra of solutions were measured in a 1 cm quartz cuvette at a repeating unit concentration of about 2.5×10^{-6} M with an optical density of 0.09–0.10 at the λ_{max}. UV–vis absorption spectra were measured with a Cary 50 UV–visible absorption spectrometer at room temperature. Fluorescence spectra were measured with a SPEX Fluorolog-τ2 fluorometer (model FL112, 450 W xenon lamp). Solution-state fluorescence spectra were obtained at a right-angle geometry using an excitation wavelength of 375 nm. Solid-state fluorescence spectra were obtained in the front-face detection geometry using an excitation wavelength of 375 nm. Time resolved fluorescence measurements were performed by exciting the samples with 160 femtosecond pulses at 390 nm from the doubled output of a Coherent RegA Ti:Sapphire amplifier. The resulting fluorescence was spectrally and temporally resolved with a Hamamatsu C4780 Streak Camera system.

Polymer films (generally, optical density = 0.09–0.12; thickness = 28–35 nm) were spin-cast on 18 × 18 mm^2 glass substrates using a WS-400 Spin Processor (Laurell Technologies Corp.) at a spin rate of 1200 rpm for 1 min, and then dried *in vacuo*. The spin-casting solutions were filtered through 0.45 μm PTFE syringe filters. Film thicknesses were measured on a M2000D Spectroscopic Ellipsometer (J. A. Woollam Co., Inc.). Uniformity of each film was confirmed by equivalent UV–vis absorption intensities from three different regions of the film.

Aggregate solutions in good solvent/poor solvent mixtures were prepared by dropwise addition of the poor solvent (H_2O) into a stirring solution of the polymer dissolved in a good solvent (THF).

Poly(vinyl alcohol)/PPE blends were prepared by quickly transferring a solution of 0.03 mg/mL *syn*-PPE_1 in 0.2 mL:2.8 mL H_2O:THF into a 1.0 mL aq. solution of 15 wt% poly(vinyl alcohol) (M_w = 31–50 kDa, 98–99% hydrolyzed) containing one drop of concentrated H_2SO_4. While stirring rapidly, a drop of 50 wt% aq. glutaric dialdehyde was immediately added to the mixture. The polymer blend was washed in 10 mL THF, then dried *in vacuo*.

Materials

All solvents were of spectral grade unless otherwise noted. Water for spectroscopic measurements was obtained from a Millipore Milli-Q purification system. $Pd(PPh_3)_4$ was purchased from Strem Chemicals, Inc. Silica gel (40–63 mm) was obtained from SiliCycle.

Compounds **1, *anti*-4, *syn*-4, 5**, and *anti*-PPE were prepared following literature procedures. All other chemicals were purchased from Aldrich Chemical Co., Inc. and used as received.

(**2**): **1**[44] (0.262 g, 0.410 mmol) and dimethyl acetylenedicarboxylate (DMAD) (0.101 mL, 0.820 mmol) were suspended in xylenes (5 mL) and stirred at 140 °C for 2.5 hours. The solvent was removed, and the product was purified by column chromatography (30:1 hexane: ethyl acetate) to afford **2** as a yellow solid (0.232 g, 72%). The spectroscopic characterization data matched those of the same compound recently synthesized in a similar manner and reported in the literature.[37] ^{1}H NMR (300 MHz, $CDCl_3$): 8.87 (2H, s), 8.01 (2H, dd, *J* = 3.3, 6.6 Hz), 7.51 (2H, dd, *J* = 3.3, 6.6 Hz), 7.48 (2H, dd, *J* = 3.0, 5.2 Hz), 7.15 (2H, dd, *J* = 3.0, 5.2 Hz), 6.23 (2H, s), 3.86 (6H, s), 1.37 (42H, s); ^{13}C NMR (75 MHz, $CDCl_3$): 165.6, 146.1, 142.3, 142.3, 132.4, 129.2, 128.6, 126.5, 126.2, 126.0, 124.5, 116.3, 102.2, 101.8, 52.7, 50.9, 19.1, 11.7; HRMS–ESI (*m/z*) for $C_{50}H_{60}O_4Si_2$ calcd $[M+H]^+$: 781.4103, found: 781.4076.

(**3**): To a solution of **2** (0.232 g, 0.297 mmol) dissolved in THF (4.0 mL), added tetrabutylammonium fluoride (1M in THF; 0.890 mL, 0.297 mmol). After stirring at room temperature overnight, the solvent was removed *in vacuo*. The crude product was purified by column chromatography (3:1 hexane: ethyl acetate) to afford **3** as a yellow solid (0.126 g, 91%). mp 110–112 °C dec. The spectroscopic characterization data matched those of the same compound recently synthesized in a similar manner and reported in the literature.[37] ^{1}H NMR (300 MHz, $CDCl_3$): 8.80 (2H, s), 8.03 (2H, dd, *J* = 3.3, 6.4 Hz), 7.55 (2H, dd, *J* = 3.2, 5.4 Hz), 7.49 (2H, dd, *J* = 3.3, 6.4), 7.14 (2H, dd, *J* = 3.2, 5.4 Hz), 6.18 (2H, s), 3.93 (2H, s), 3.85 (6H, s); ^{13}C NMR (75 MHz, $CDCl_3$): 165.8, 145.7, 142.7, 142.0, 132.5, 129.0, 128.5, 126.4, 125.8, 124.7, 115.4, 87.4, 79.00, 52.8, 50.6; HRMS–ESI (*m/z*) for $C_{32}H_{20}O_4$ calcd $[M+H]^+$: 469.1434, found: 469.1450.

Polymers *anti*-PPE, *syn*-PPE, and *syn*-PPE_y: These polymers were prepared similarly, and a general procedure is illustrated by the following synthesis of *syn*-PPE_1. To a 25 mL Schlenk tube, added **5**[36] (20.3 mg, 2.81×10^{-5} mol), ***syn*-4**[36] (17.8 mg, 2.92×10^{-5} mol), and **3** (16.3 μL of a 17.9 mM $CHCl_3$ solution, 2.92×10^{-7} mol). The solvent was evaporated at 35 °C under a flow of nitrogen, and then the mixture was dried *in vacuo*. Under a nitrogen atmosphere, $Pd(PPh_3)_4$ (3.3 mg, 2.8×10^{-6} mol) and CuI (3.2 mg, 1.7×10^{-5} mol) were added. The vessel was evacuated and back-filled with argon three times, followed by the addition of degassed 7:3 toluene: diisopropylamine (1.5 mL). The mixture was stirred at 70 °C for 3 days under an argon atmosphere. The mixture was then subjected to a work up with $CHCl_3$ and a sat. aq. NH_4Cl solution. The organic phase was washed with water, and then brine. The organic extract was dried over $MgSO_4$ and filtered prior to solvent removal under reduced pressure. The residue was dissolved in $CHCl_3$, and then added dropwise in rapidly stirred methanol. The mixture was centrifuged at 2500 rpm for 30 min and then decanted. The polymer was then washed with additional MeOH, and the mixture was centrifuged and decanted again. The solid polymer was then dissolved in acetone, transferred to a vial, then dried *in vacuo* to afford a yellow solid (25.7 mg, ~78%). M_n = 21 kDa, PDI = 2.14. ^{1}H NMR (500 MHz, $CDCl_3$): 8.50−8.46 (1H, br), 8.28−8.22 (1H, br), 8.12 (0.11H, s), 8.01 (0.10H, d, *J* = 8.4 Hz), 7.81 (0.13H, d, *J* = 8.4 Hz), 7.70−7.54 (0.55H, br), 7.50−7.39 (4H, br), 7.16−6.99 (4H br), 6.10−5.96 (4H, br), 3.92−3.83 (12H, br). ATR–IR (ν/cm^{-1}): 2958, 2852, 1724, 1641, 1512, 1437, 1211, 1144, 1063, 814, 750, 677.

syn-PPE_9: Reagents: **5**[36] (24.9 mg, 3.45×10^{-5} mol), ***syn*-4**[36] (19.9 mg, 3.26×10^{-5} mol), **3** (181 μL of a 17.9 mM $CHCl_3$ solution, 3.26×10^{-6} mol), $Pd(PPh_3)_4$ (4.0 mg, 3.5×10^{-6} mol) and CuI (3.9 mg, 2.0×10^{-5} mol), 7:3 toluene: diisopropylamine (4.2 mL). Yield: 29.8 mg (~74%). M_n = 13 kDa, PDI = 1.95. ^{1}H NMR (500 MHz, $CDCl_3$): 8.52−8.46 (1H, br), 8.28 −8.24 (1H, br), 8.13 (0.26H, s), 8.02 (0.17H, d, *J* = 8.3 Hz), 7.82 (0.16H, d, *J* = 8.3 Hz), 7.68

−7.56 (0.88H, br), 7.48−7.36 (4H, br), 7.18−6.98 (4H br), 6.10−5.96 (4H, br), 3.93−3.82 (12H, br). ATR–IR (ν/cm^{-1}): 2956, 2848, 1724, 1641, 1510, 1437, 1209, 1144, 1061, 818, 750, 677.

syn-PPE Reagents: **5**[36] (45.5 mg, 6.30 × 10^{-5} mol), ***syn*-4**[36] (40.5 mg, 6.63 × 10^{-5} mol), Pd(PPh$_3$)$_4$ (4.0 mg, 3.5 × 10^{-6} mol), CuI (5.0 mg, 2.6 × 10^{-5} mol), 7:3 toluene: diisopropylamine (2.0 mL). Yield: 63.9 mg (87%). M_n = 28 kDa, PDI = 4.92. ^{1}H NMR (500 MHz, $CDCl_3$): 8.50−8.46 (1H, br), 8.28−8.22 (1H, br), 8.12 (0.07H, s), 8.01 (0.07H, d, J = 8.6 Hz), 7.82 (0.09H, d, J = 8.6 Hz), 7.72−7.54 (0.90H, br), 7.52−7.36 (4H, br), 7.22−6.98 (4H br), 6.10−5.96 (4H, br), 3.92−3.81 (12H, br). ATR-IR (ν/cm^{-1}): 2958, 2852, 1726, 1641, 1514, 1437, 1209, 1144, 1063, 820, 752, 677.

anti-PPE: Reagents: **5**[36] (107 mg, 1.48 × 10^{-4} mol), ***anti*-4**[36] (95.2 mg, 1.56 × 10^{-4} mol), Pd(PPh$_3$)$_4$ (17.1 mg, 1.5 × 10^{-5} mol), CuI (16.9 mg, 8.9 × 10^{-5} mol), 7:3 toluene: diisopropylamine (5.0 mL). Yield: 143.4 mg (83%). M_n = 39 kDa, PDI = 2.99. The spectroscopic characterization data was consistent with that reported previously for the same polymer.[36,38] ^{1}H NMR (500 MHz, $CDCl_3$): 8.48−8.44 (1H, br), 8.29−8.22 (1H, br), 8.12 (0.07H, s), 8.02 (0.04H, d, J = 8.5 Hz), 7.82 (0.04H, d, J = 8.5 Hz), 7.72−7.64 (0.20H, br), 7.55−7.42 (4H, br), 7.18−7.08 (4H br), 6.10−5.95 (4H, br), 3.88−3.80 (12H, br). ATR–IR (ν/cm^{-1}): 2958, 2850, 1726, 1641, 1510, 1437, 1209, 1144, 1061, 808, 750, 694.

Thermally degraded *anti*-PPE: Heated *anti*-PPE (8.0 mg) in a TGA Q50 (TA Instruments) at a temperature ramp rate of 5 °C/min from room temperature to 300 °C, under a helium flow rate of 90 mL/min. After cooling to room temperature, the degraded polymer was transferred to a vial, and chloroform was added. The chloroform-soluble portion was filtered through a 0.45 μm PTFE syringe filter, then dried *in vacuo* to afford a yellow solid (M_n = 35 kDa, PDI = 2.85). ^{1}H NMR (500 MHz, $CDCl_3$): 8.48−8.43 (1H, br), 8.29−8.23 (1H, br), 8.12 (0.11H, s), 8.01 (0.07H, d, J = 8.7 Hz), 7.81 (0.02H, d, J = 8.7 Hz), 7.68−7.65 (0.13H, br), 7.55−7.43 (4H, br), 7.18−7.05 (4H br), 6.09−5.95 (4H, br), 3.88−3.80 (12H, br). ATR–IR (ν/cm^{-1}): 2956, 2925, 2854, 1726, 1641, 1512, 1437, 1211, 1144, 1061, 808, 752, 694.

Thermally degraded *syn*-PPE: Heated *syn*-PPE (4.7 mg) in a TGA Q50 (TA Instruments) at a temperature ramp rate of 5 °C/min from room temperature to 250 °C, under a helium flow rate of 90 mL/min. After cooling to room temperature, the degraded polymer was transferred to a vial, and chloroform was added. The chloroform-soluble portion was filtered through a 0.45 μm PTFE syringe filter, then dried *in vacuo* to afford a yellow solid (M_n = 20 kDa, PDI = 2.04). ^{1}H NMR (500 MHz, $CDCl_3$): 8.51−8.44 (1H, br), 8.29−8.22 (1H, br), 8.12 (0.16H, s), 8.01 (0.10H, d, J = 8.8 Hz), 7.81 (0.04H, d, J = 8.8 Hz), 7.70−7.56 (0.39H, br), 7.55−7.38 (4H, br), 7.12−7.00 (4H br), 6.08−5.95 (4H, br), 3.92−3.83 (12H, br). ATR–IR (ν/cm^{-1}): 2958, 2929, 2856, 1724, 1641, 1512, 1437, 1213, 1146, 1063, 804, 754, 677.

Supplementary Material

Refer to Web version on PubMed Central for supplementary material.

Acknowledgments

We are thankful to Y. Kim for providing compound **1**, and we also thank J. Bouffard, A.J. McNeil, and E. Ishow for helpful discussions. This work was supported by the Institute for Soldier Nanotechnologies under Contract DAAD-19-02-0002 with the U.S. Army Research Office and NIH grant 1-U01-HL080731 (project 4).

References

1. Burroughes JH, Bradley DDC, Brown AR, Marks RN, Mackay K, Friend RH, Burn PL, Holmes AB. Nature 1990;347:539.

2. Rees ID, Robinson KL, Holmes AB, Towns CR, O'Dell R. MRS Bull 2002;27:451–455.
3. Fukuda M, Sawada K, Morita S, Yoshino K. Synth Met 1991;41:855–858.
4. Leclerc M. J Polym Sci, Part A: Polym Chem 2001;39:2867–2873.
5. Kreyenschmidt M, Klaerner G, Fuhrer T, Ashenhurst J, Karg S, Chen WD, Lee VY, Scott JC, Miller RD. Macromolecules 1998;31:1099–1103.
6. Bliznyuk VN, Carter SA, Scott JC, Klarner G, Miller RD, Miller DC. Macromolecules 1999;32:361–369.
7. Turro, NJ. Modern Molecular Photochemistry. University Science Books; Sausalito, CA: 1991.
8. Gilbert, A.; Baggott, JE. Essentials of Molecular Photochemistry. Blackwell Scientific Publications; Boston: 1991.
9. For a review, see: Conwell E. Trends Polym Sci 1997;5:218–222.222
10. Yamamoto T, Maruyama T, Ikeda T, Sisido M. J Chem Soc, Chem Commun 1990:1306–1307.
11. Jenekhe SA, Osaheni JA. Science 1994;265:765–768. [PubMed: 17736274]
12. Yamamoto T, Suganuma H, Saitoh Y, Maruyama T, Inoue T. Jpn J Appl Phys, Part 2 1996;35:L1142–L1144.
13. Stampfl J, Graupner W, Leising G, Scherf U. J Lumin 1995;63:117–123.
14. Samuel IDW, Rumbles G, Collison CJ. Phys Rev B 1995;52:11573–11576.
15. Kim Y, Bouffard J, Kooi SE, Swager TM. J Am Chem Soc 2005;127:13726–13731. [PubMed: 16190739]
16. Levitsky IA, Kim J, Swager TM. J Am Chem Soc 1999;121:1466–1472.
17. List EJW, Guentner R, de Freitas PS, Scherf U. Adv Mater 2002;14:374–378.
18. Lupton JM, Craig MR, Meijer EW. Appl Phys Lett 2002;80:4489–4491.
19. Zojer E, Pogantsch A, Hennebicq E, Beljonne D, Bredas JL, de Freitas PS, Scherf U, List EJW. J Chem Phys 2002;117:6794–6802.
20. Franco I, Tretiak S. Chem Phys Lett 2003;372:403–408.
21. Gaal M, List EJW, Scherf U. Macromolecules 2003;36:4236–4237.
22. Hintschich SI, Rothe C, Sinha S, Monkman AP, de Freitas PS, Scherf U. J Chem Phys 2003;119:12017–12022.
23. List EJW, Gaal M, Guentner R, de Freitas PS, Scherf U. Synth Met 2003;139:759–763.
24. Nikitenko VR, Lupton JM. J Appl Phys 2003;93:5973–5977.
25. Romaner L, Pogantsch A, de Freitas PS, Scherf U, Gaal M, Zojer E, List EJW. Adv Funct Mater 2003;13:597–601.
26. Yang XH, Neher D, Spitz C, Zojer E, Bredas JL, Guntner R, Scherf U. J Chem Phys 2003;119:6832–6839.
27. Kulkarni AP, Kong XX, Jenekhe SA. J Phys Chem B 2004;108:8689–8701.
28. Chi CY, Im C, Enkelmann V, Ziegler A, Lieser G, Wegner G. Chem Eur J 2005;11:6833–6845.
29. Becker K, Lupton JM, Feldmann J, Nehls BS, Galbrecht F, Gao DQ, Scherf U. Adv Funct Mater 2006;16:364–370.
30. Samuel IDW, Crystall B, Rumbles G, Burn PL, Holmes AB, Friend RH. Chem Phys Lett 1993;213:472–478.
31. Yan M, Rothberg L, Hsieh BR, Alfano RR. Phys Rev B 1994;49:9419–9422.
32. McQuade DT, Pullen AE, Swager TM. Chem Rev 2000;100:2537–2574. [PubMed: 11749295]
33. Rose A, Lugmair CG, Swager TM. J Am Chem Soc 2001;123:11298–11299. [PubMed: 11697976]
34. Thomas SW, Joly GD, Swager TM. Chem Rev 2007;107:1339–1386. [PubMed: 17385926]
35. Nelson J. Curr Opin Solid State Mater Sci 2002;6:87–95.
36. Kim Y, Whitten JE, Swager TM. J Am Chem Soc 2005;127:12122–12130. [PubMed: 16117554]
37. Ishow E, Bouffard J, Kim Y, Swager TM. Macromolecules 2006;39:7854–7858.
38. Kim, Y. PhD Thesis. Massachusetts Institute of Technology; 2005.
39. Swager TM, Gil CJ, Wrighton MS. J Phys Chem 1995;99:4886–4893.

40. Hennebicq E, Pourtois G, Scholes GD, Herz LM, Russell DM, Silva C, Setayesh S, Grimsdale AC, Mullen K, Bredas JL, Beljonne D. J Am Chem Soc 2005;127:4744–4762. [PubMed: 15796541]
41. Flory, PJ. Principles of Polymer Chemistry. Cornell University Press; Ithaca: 1953.
42. Pritchard, JG. Poly(Vinyl Alcohol): Basic Properties and Uses. Macdonald & Co; London: 1970.
43. Finch, CA. Polyvinyl Alcohol: Developments. Wiley; New York: 1992.
44. Anthony JE, Brooks JS, Eaton DL, Parkin SR. J Am Chem Soc 2001;123:9482–9483. [PubMed: 11562247]

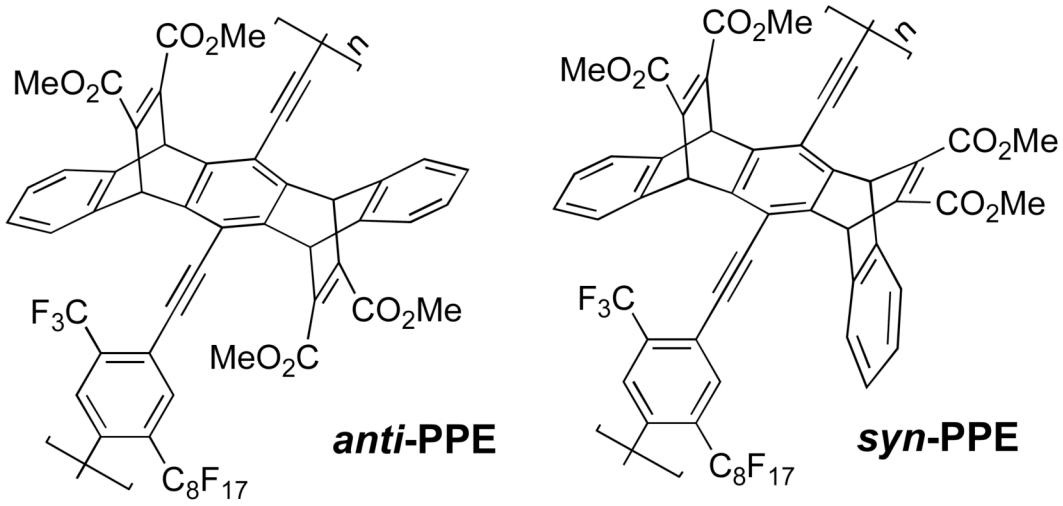

Figure 1.
Structures of *anti*-PPE and *syn*-PPE.[15]

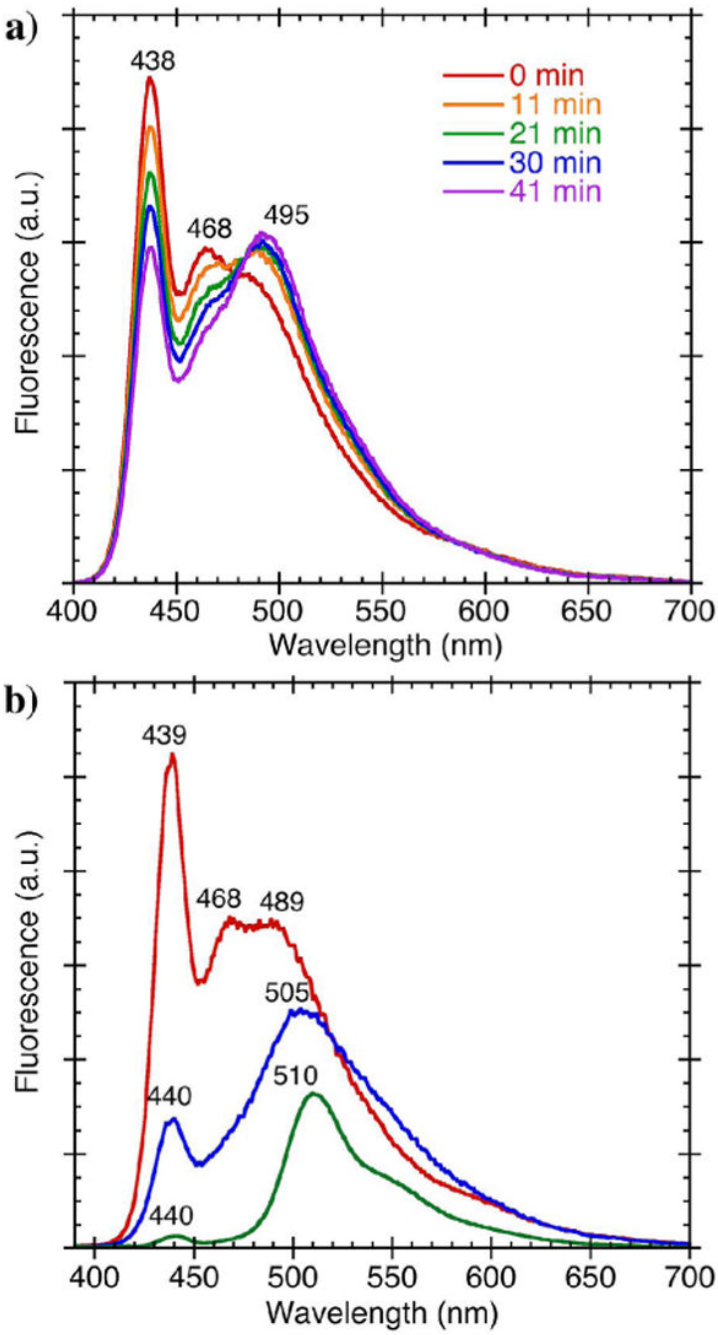

Figure 2.

(a) Fluorescence spectra of an *anti*-PPE spin-cast film (optical density, OD = 0.24), upon photoirradiation with a fluorometer (excitation wavelength λ_{ex} = 375 nm, bandpass = 2.5 nm) in an ambient air atmosphere. (b) Fluorescence spectra (λ_{ex} = 375 nm) of *anti*-PPE spin-cast films, before (red) and after (blue) the film (OD = 0.23) was irradiated for 3.5 minutes with a UVP Pen Ray mercury lamp (254 nm) in an inert nitrogen (glovebox) atmosphere. Green line: fluorescence spectrum (λ_{ex} = 375 nm) of a spin-cast film (OD = 0.12) of a sample of *anti*-PPE that was previously heated to 300 °C in an inert helium atmosphere.

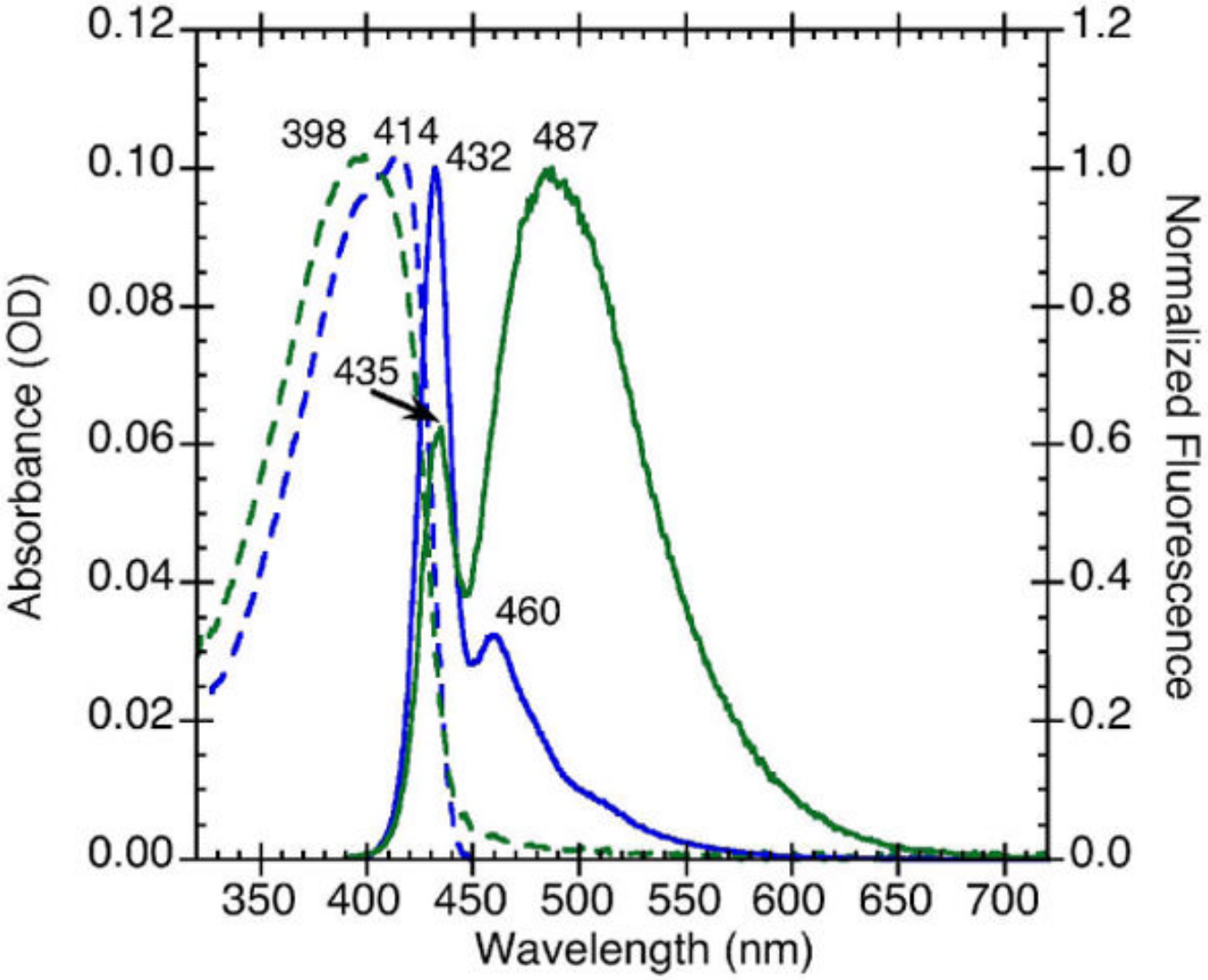

Figure 3.
Absorption (dashed) and normalized fluorescence (solid) spectra of *syn*-PPE in chloroform solution (blue) and as a spin-cast film (green). Fluorescence spectra were obtained using an excitation wavelength λ_{ex} = 375 nm.

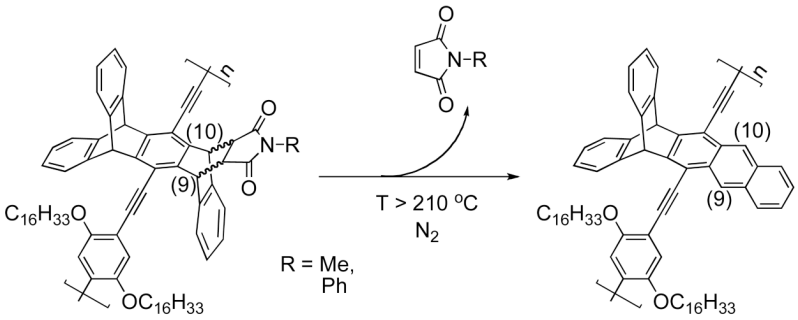

Figure 4.
Proposed retro-Diels–Alder reaction in a PPE containing a [2.2.2] bicyclic ring system.[37]

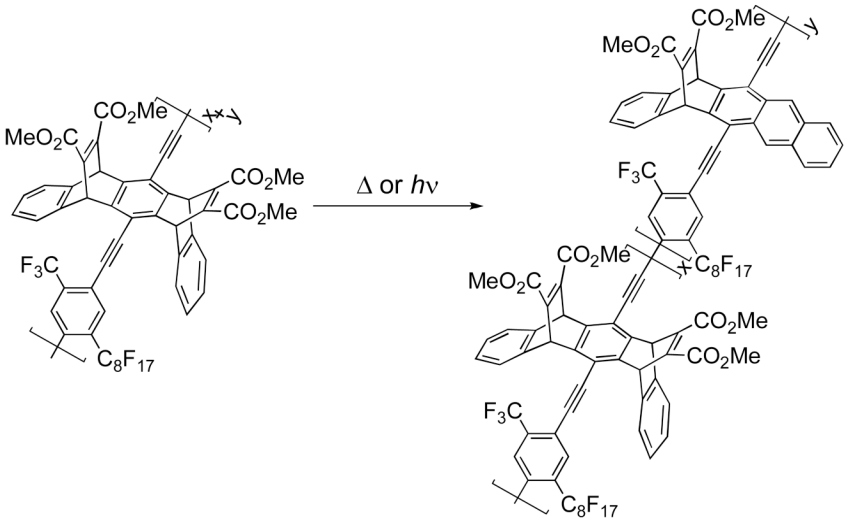

Figure 5.
Proposed degradation product from the photoirradiation or heating of *syn*-PPE.

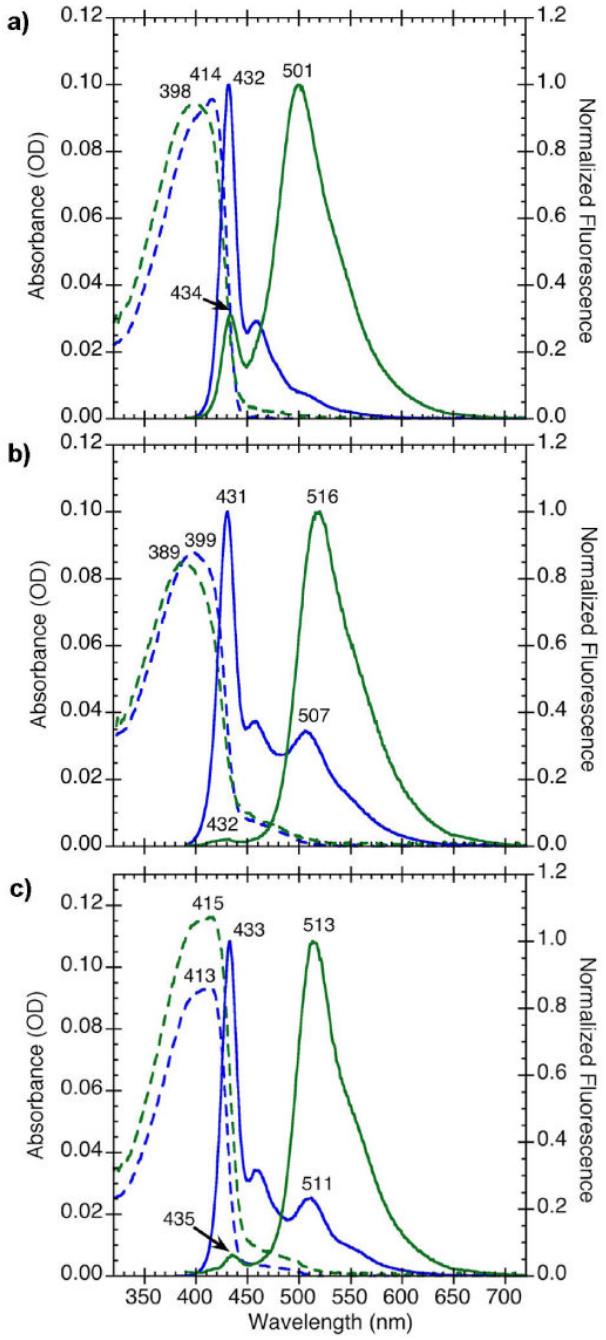

Figure 6.

Absorption (dashed) and normalized fluorescence (solid) spectra of (a) *syn*-PPE_1, (b) *syn*-PPE_9, and (c) thermally degraded *syn*-PPE in chloroform solution (blue) and as spin-cast films (green). Fluorescence spectra were obtained using an excitation wavelength λ_{ex} = 375 nm.

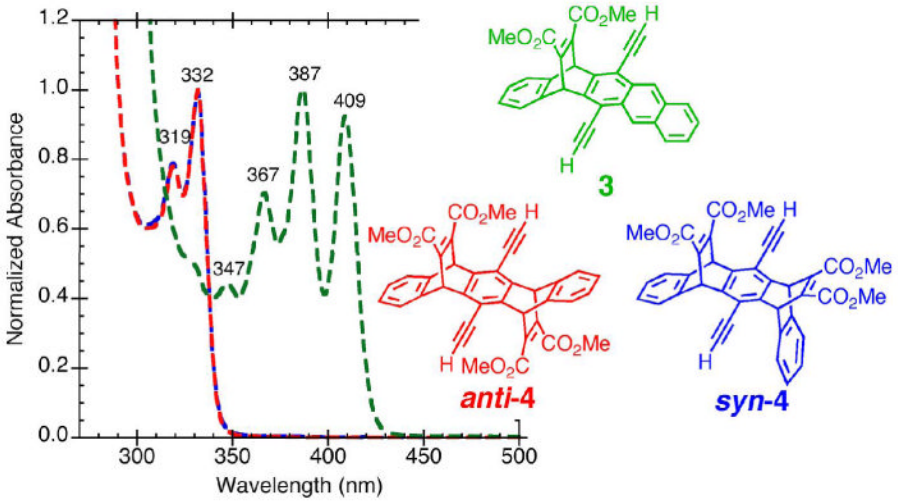

Figure 7.
Normalized absorption spectra of the anthryl monomer **3** (green), ***anti*-4** (red), and ***syn*-4** (blue) dissolved in chloroform.

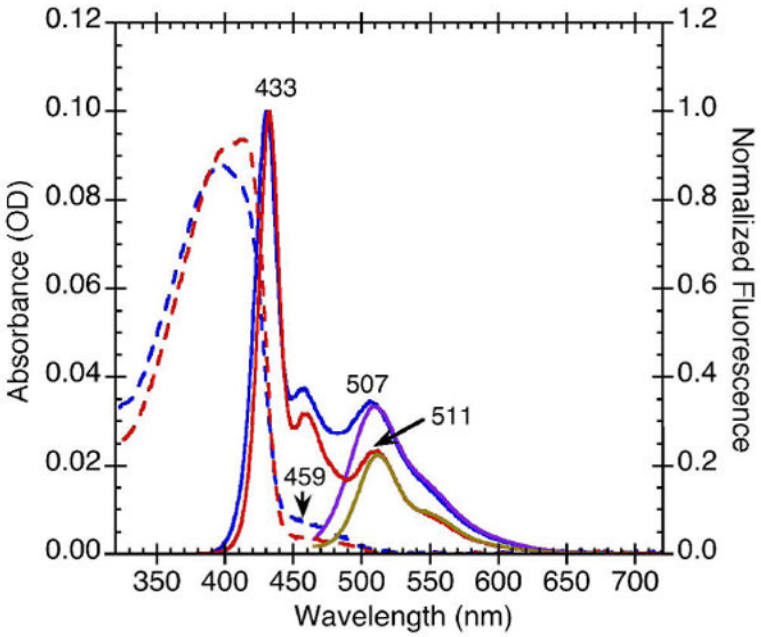

Figure 8.

Absorption (dashed) and normalized fluorescence (solid) spectra of *syn*-PPE_9 (blue) and thermally degraded *syn*-PPE (red) in chloroform solution. Fluorescence spectra were obtained using an excitation wavelength λ_{ex} = 375 nm. The low-energy fluorescence spectra of each polymer were obtained by excitation at 459 nm (purple and brown, respectively).

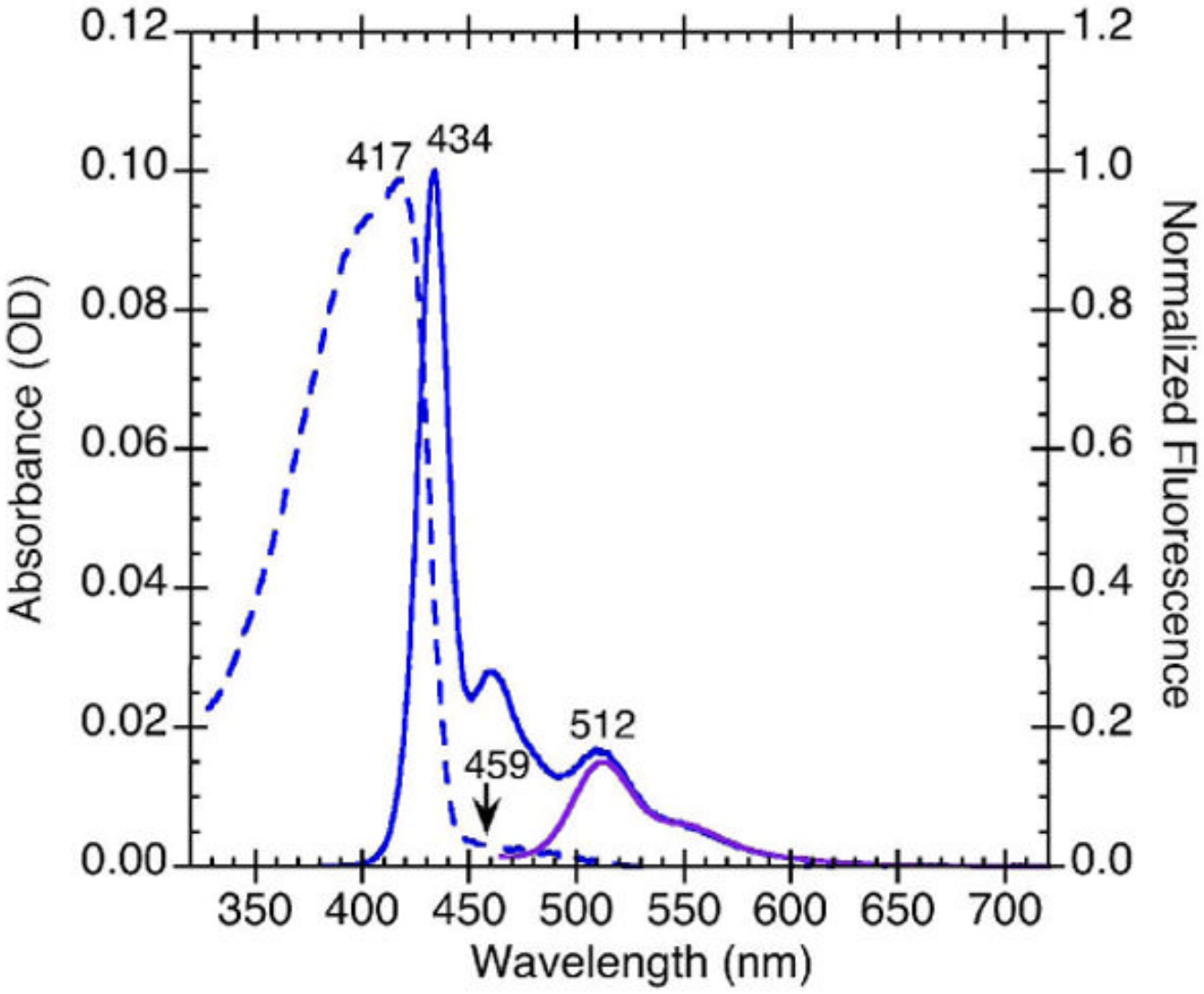

Figure 9.

Absorption (dashed) and normalized fluorescence (solid) spectra of thermally degraded *anti*-PPE (blue) in chloroform solution. The fluorescence spectrum was obtained using an excitation wavelength λ_{ex} = 375 nm. The low-energy fluorescence spectrum (purple) was obtained by excitation at 459 nm.

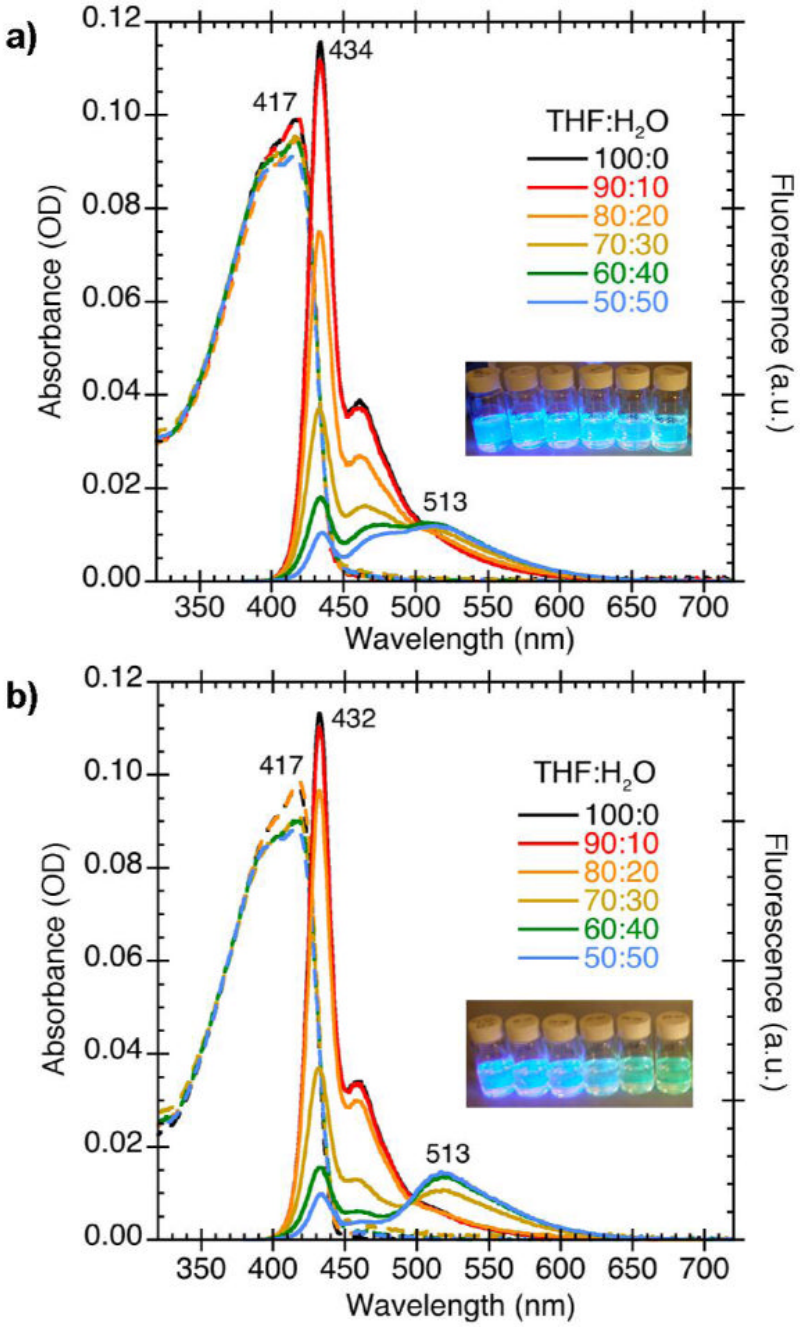

Figure 10.

Absorption (dashed) and fluorescence (solid) spectra of (a) *syn*-PPE and (b) *syn*-PPE_1 in solutions of tetrahydrofuran: water (v:v). Fluorescence spectra were obtained using an excitation wavelength λ_{ex} = 375 nm. Insets: fluorescence photographs of the solutions in order of increasing aggregation from left to right, irradiated with a 365 nm lamp.

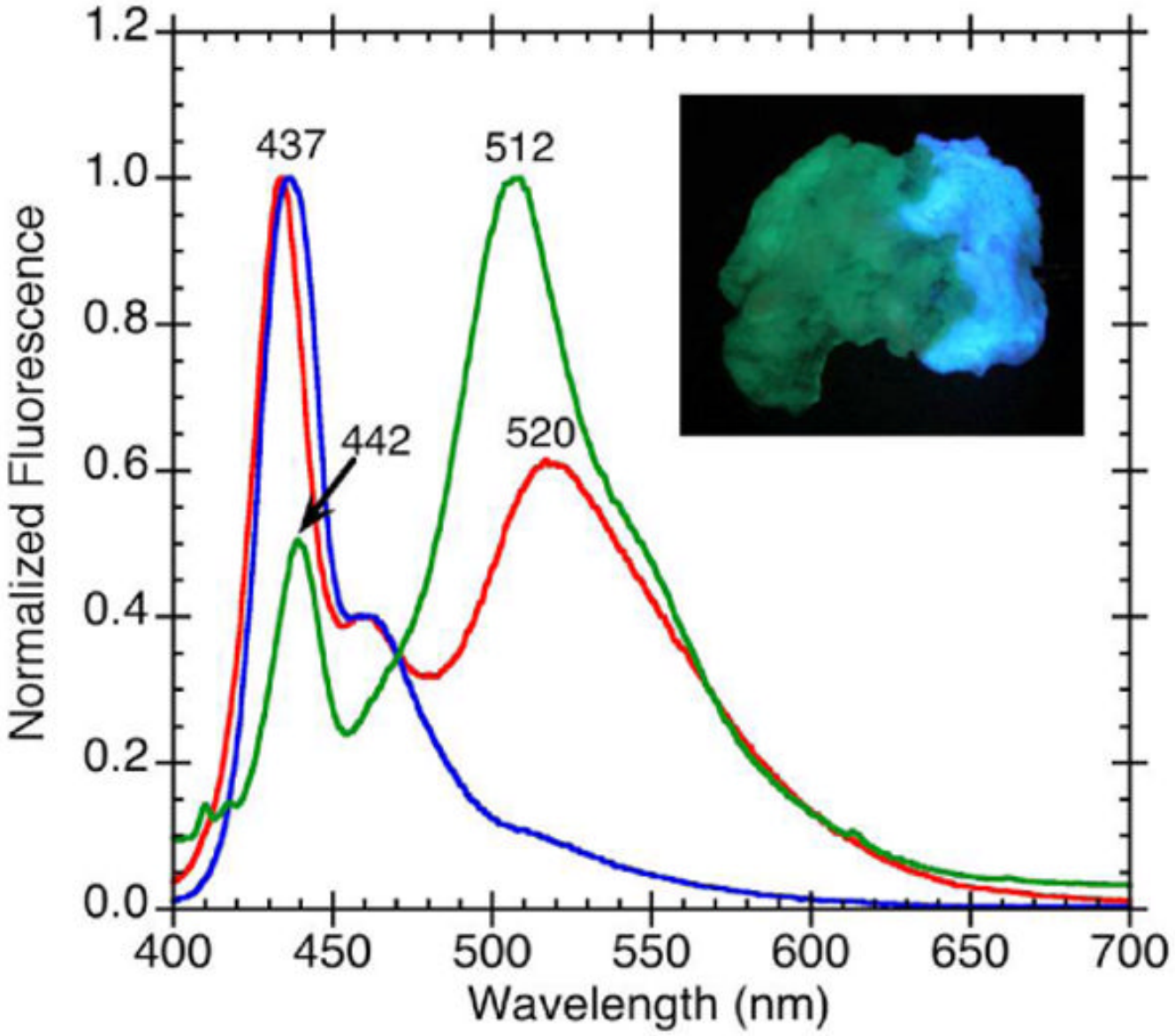

Figure 11.

Normalized fluorescence spectra (λ_{ex} = 375 nm) of a blend of PVA and *syn*-PPE_1 immediately after sample preparation (red), after washing in THF and drying *in vacuo* (blue), and after submerging in H_2O (green). Inset: fluorescence photograph of a PVA/PPE blend that was only partially submerged in H_2O, irradiated with a 365 nm lamp.

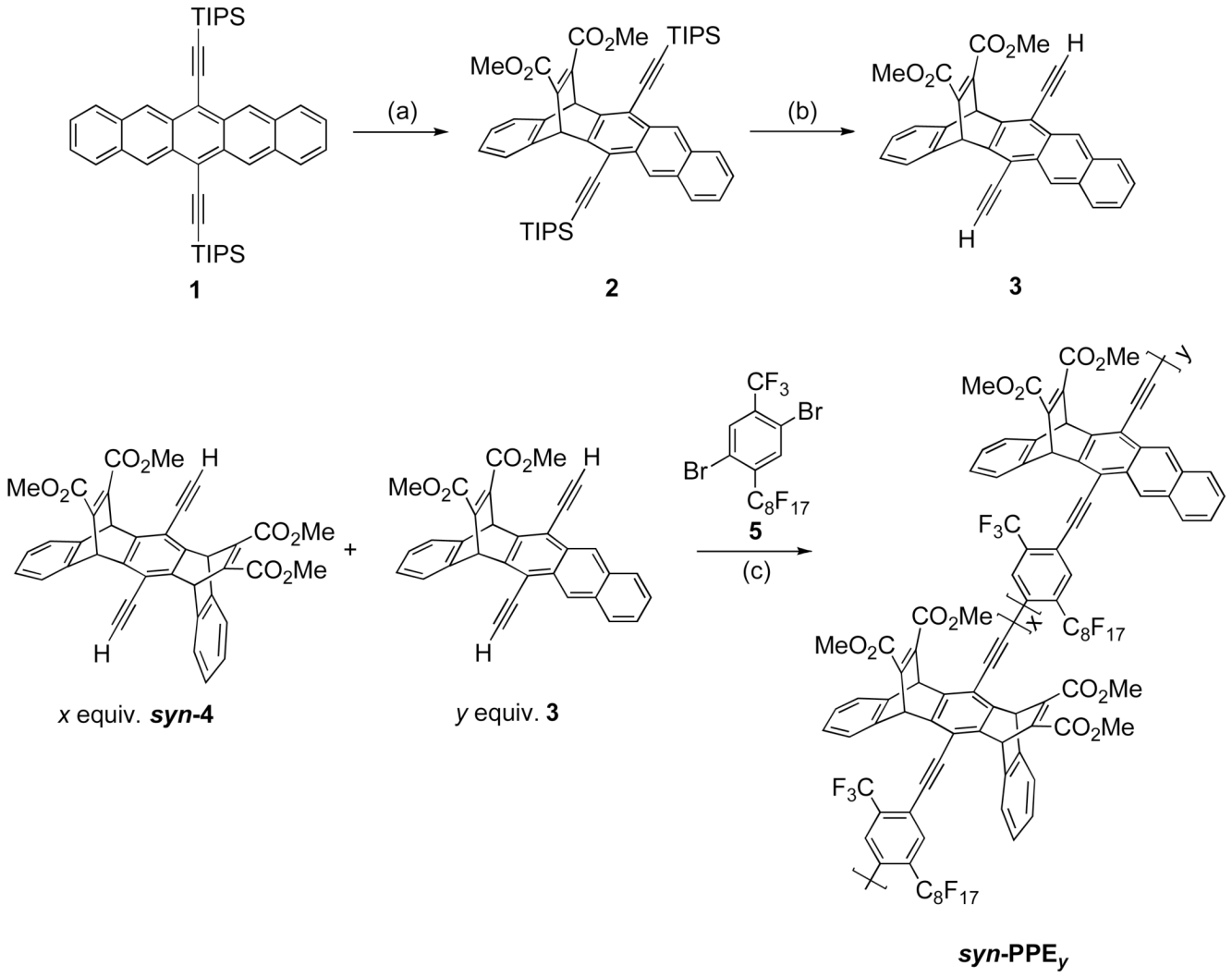

Scheme 1. Synthesis of the Model Degradation Polymers *syn*-PPE$_y$[a]

[a] (a) DMAD, xylenes, 140 °C; (b) TBAF, THF, rt; (c) Pd(PPh$_3$)$_4$, CuI, PhMe, *i*Pr$_2$NH, 70 °C.

Table 1

^{1}H NMR Integration Ratios for the *anti*- and *syn*-PPEs[a]

Polymer	M_n (kDa)	% anthryl comonomer	*R*(8.1/6.0)
anti-PPE	39	0	0.018
syn-PPE	28	0	0.018
syn-PPE_1	21	1	0.027
syn-PPE_9	13	9	0.066
thermally degraded *anti*-PPE	35	n/a	0.029
thermally degraded *syn*-PPE	20	n/a	0.039

[a] *R*(8.1/6.0) denotes the NMR integration ratio of the proton resonance signal around 8.1 ppm to the proton resonance signal around 6.0 ppm.

Table 2

Summary of Optical Properties of *syn*-PPE$_y$ Copolymers

Polymer	Absorption[a] λ_{max} (nm)		Fluorescence[b] λ_{max} (nm) / Excited State Lifetime (ns)		
	In $CHCl_3$	Film	In $CHCl_3$	Film	I_{green}/I_{blue}[c]
syn-PPE	414 nm	398 nm	432 nm / 0.37 ns	432 nm / < 0.05 ns 487 nm / 0.54 ns (73%), 1.5 ns (27%)	1.6
syn-PPE$_1$	414 nm	398 nm	432 nm / 0.38 ns	434 nm / < 0.05 ns 501 nm / 0.90 ns (60%), 1.9 ns (40%)	3.2
syn-PPE$_9$	399 nm, shoulder > 450 nm	389 nm, shoulder > 450 nm	431 nm / 0.41 ns 507 nm / 0.43 ns (81%), 1.8 ns (19%)	432 nm / < 0.05 ns 516 nm / 0.83 ns (56%), 1.8 (44%)	46
thermally degraded *syn*-PPE	413 nm, shoulder > 450 nm	415 nm, shoulder > 450 nm	433 nm / 0.44 ns 511 nm / 1.6 ns	435 nm / < 0.05 ns 513 nm / 0.61 ns (74%), 1.8 ns (26%)	16

[a] Absorption spectra matched the excitation spectra in both solution state and solid state (obtained using emission wavelengths = 510–535 nm).

[b] Fluorescence spectra were obtained using an excitation wavelength λ_{ex} = 375 nm.

[c] For films, I_{green}/I_{blue} is the ratio of green band (~500 nm) maximum fluorescence intensity to the blue band (~432 nm) maximum fluorescence intensity.